



Driven magnetic reconnection in the COMPASS-C tokamak

A. W. Morris, P. G. Carolan, R. Fitzpatrick, T. C. Hender, and T. N. Todd

Citation: *Physics of Fluids B: Plasma Physics (1989-1993)* **4**, 413 (1992); doi: 10.1063/1.860291

View online: <http://dx.doi.org/10.1063/1.860291>

View Table of Contents: <http://scitation.aip.org/content/aip/journal/pofb/4/2?ver=pdfcov>

Published by the [AIP Publishing](#)

Articles you may be interested in

[Plasma density measurements on COMPASS-C tokamak from electron cyclotron emission cutoffs](#)
Rev. Sci. Instrum. **67**, 462 (1996); 10.1063/1.1146613

[Spontaneous and driven perpendicular rotation in tokamaks](#)
Phys. Fluids B **5**, 2519 (1993); 10.1063/1.860738

[Poloidal magnetic field dependence of the edge electric field layer width in the H mode in tokamaks](#)
Phys. Fluids B **4**, 290 (1992); 10.1063/1.860276

[ICRH in large tokamaks with poloidal magnetic field](#)
AIP Conf. Proc. **190**, 282 (1989); 10.1063/1.38503

[Diagnostic instrument for the measurement of poloidal magnetic fields in tokamaks](#)
Rev. Sci. Instrum. **57**, 1552 (1986); 10.1063/1.1138583

Driven magnetic reconnection in the COMPASS-C tokamak

A. W. Morris, P. G. Carolan, R. Fitzpatrick, T. C. Hender, and T. N. Todd
AEA Fusion, Culham Laboratory (UKAEA/Euratom Fusion Association), Abingdon, Oxon, England

(Received 30 August 1991; accepted 22 October 1991)

The question of the influence of nonaxisymmetric field perturbations on tokamaks is investigated. Recent experiments in the COMPASS-C tokamak [in *Proceedings of the 15th Symposium on Fusion Technology*, Utrecht (North-Holland, Amsterdam, 1989), Vol. 1, p. 361] with externally applied helical fields reveal that magnetic islands do not appear until the applied field exceeds a certain value, when plasma rotation and confinement are affected. A new resistive magnetohydrodynamic model including plasma rotation now provides an explanation of this threshold, and is quantitatively consistent with experimental results in Ohmic plasmas. The results indicate the tolerable error fields in future tokamaks. The effects of perturbations with various poloidal and toroidal mode numbers have been studied.

I. INTRODUCTION

Field errors do and will exist at some level on all present and future tokamaks. These can arise from a variety of sources including misalignments of the poloidal and toroidal field coils, magnetic materials (e.g., in building girders or ancillary equipment), and eddy currents in the structures. It has been observed experimentally, on DIII-D, for example,¹ that the presence of nonaxisymmetric magnetic field errors can lead to degraded performance, amongst a number of other effects. Many experiments have been performed to study the effect of resonant magnetic perturbations (RMP's) on tokamak discharges, starting with the Pulsator² and ATC³ experiments in the mid-1970s and continuing to the present.⁴⁻⁸ It has been realized for some time^{4,9} that it is not in general appropriate to calculate magnetic island widths by superposing the error fields calculated *in vacuo*, B_r^{vac} , on the equilibrium magnetic field; rather the plasma response should be included, although this knowledge has seldom been applied to experiments. Recent theoretical work¹⁰ shows that plasma rotation also plays a key role in the impact of error fields on tokamaks. To investigate these issues a series of experiments has been performed on COMPASS-C¹¹ to study, in a controlled fashion, the effects of RMP's on a variety of discharges. The theoretical model¹⁰ allows predictions to be made for future large devices, such as the International Thermonuclear Experimental Reactor (ITER¹²), and the COMPASS-C data permit this model to be extensively tested. A more complete discussion of the results is in preparation.

II. EXPERIMENTAL RESULTS AND INTERPRETATION

COMPASS-C (now being replaced by COMPASS-D) had major radius $R = 0.557$ m, minor radius $a = 0.196$ m, plasma current $I_p \lesssim 200$ kA, and toroidal field $B_\phi \lesssim 1.75$ T and was equipped with a comprehensive set of external conductors for the generation of a wide variety of magnetic field perturbations.⁶ Sensitive magnetic pickup coils were used for the detection of quasistationary helical structures and changes as low as 0.1 G outside the vessel could be measured, the poloidal field coils having been aligned to

reduce error fields to below 0.5 G (toroidal mode number $n = 1$).¹³ A high-resolution Doppler spectrometer allows measurements of the toroidal velocity v_ϕ^{imp} of boron³⁺ (BIV) impurity ions in Ohmic plasmas with good time and velocity resolution, ~ 100 μsec and 1 km sec^{-1} (equivalent to 0.3 kHz for $n = 1$ modes), respectively. COMPASS-C had been boronized and conditioned by glow discharge cleaning in helium prior to the hydrogen and deuterium experiments described here, allowing access to the low-density regime required for this work.

A. Field perturbations with $m=2$, $n=1$

Figure 1(a) shows the main effects to be discussed. An RMP, with poloidal and toroidal mode numbers $m = 2$, $n = 1$ (predominantly), is applied during the flat-top portion of an Ohmic discharge with $q_\psi(a) \simeq 4.3$ and a low level of magnetohydrodynamic (MHD) activity. It is seen that there is little effect until a certain helical current is reached, corresponding to $B_r^{\text{vac}}(2,1) = 19$ G at the limiter ($B_r^{\text{vac}}/B_\theta = 2\%$) in this case. There is then a dramatic change in the soft-x-ray flux, and the toroidal plasma rotation v_ϕ^{imp} reverses. Modeling indicates that BIV radiation derives from a zone about 5 cm radially in from the limiter, 2-4 cm outside the $q = 2$ surface. A reduction in τ_E (diamagnetic) is also observed which may be as great as $\sim 40\%$, and there is a concomitant rise in the loop voltage (I_p is feedback controlled). Reductions in the ion temperature (from neutral particle analysis of H and D temperatures, and the Doppler spectrometer measuring BIV) are typically $\lesssim 10\%$ so that most of the $\sim 30\%$ drop in energy (in this case) is due to changes in the electron energy content. This event (termed "penetration") is consistent with the appearance of a magnetic island, as explained below. More details are shown in Fig. 1(b). Here the $B_r^p(n=1)$ signal is the difference between the total field and the vacuum field at a locked mode detector (two saddle loops of extent $\Delta\theta \simeq 45^\circ$, $\Delta\phi \simeq 70^\circ$ at $r = 0.29$ m and 180° apart toroidally) and it is this signal that shows the appearance of the magnetic island at 128 msec. As the RMP is removed, the static mode structure starts to rotate, when it is determined to be predominantly $m = 2$ from an

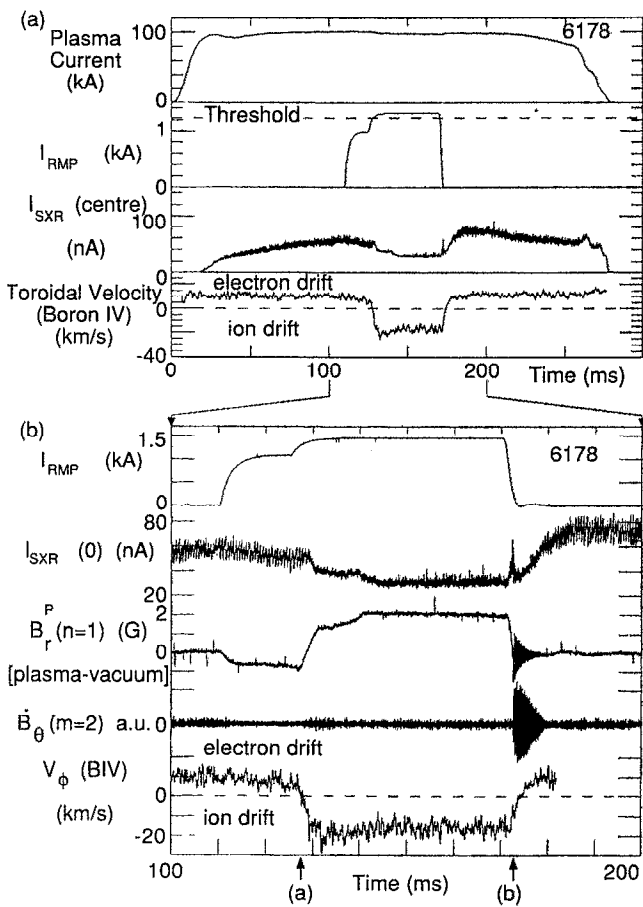


FIG. 1. (a) Penetration of applied $m = 2, n = 1$ RMP on COMPASS-C. $B_\phi = 1.1$ T, $q_\phi(a) = 4.25$, $\bar{n}_e = 1.2 \times 10^{19} \text{ m}^{-3}$, $B_r^{2,1}(a) = 14 \times I_{\text{RMP}} \text{ (kA)}$ G. Note the reversal of rotation and loss of confinement. (b) Expanded traces for the same shot. Note the change in B_r at (a) the time of penetration (128 msec), and (b) the unlocking mode. The changes in v_ϕ are seen to coincide with the penetration and unlocking events. $v_\phi > 0$ corresponds to rotation with the electron drift, $-J_\phi/en_e$.

array of Mirnov coils just outside the limiter radius, so it is presumed that the stationary mode is also primarily $m = 2, n = 1$, although an $m = 1$ component is sometimes indicated by soft-x-ray signals. The mode frequency increases to the normal $m = 2$ frequency on COMPASS-C, ~ 14 kHz, on a time scale ~ 4 msec, similar to the global energy confinement time, which has in turn been found to be similar to the global momentum confinement time on most tokamaks.

B. Interpretation and simple model of penetration

Figure 1(b) shows that the presence of plasma initially reduces $B_r(n = 1)$ below the vacuum field but when the "penetration" event occurs, $B_r(n = 1)$ exceeds B_r^{vac} ("amplification"). How this is related to the appearance of a magnetic island may be understood in terms of a simple MHD model. When there is an applied RMP, but no magnetic island, $B_r(2, 1)$ is zero at the resonant surface ($r = r_s$). This means that the radial field eigenfunction $B_r(r)$ is ev-

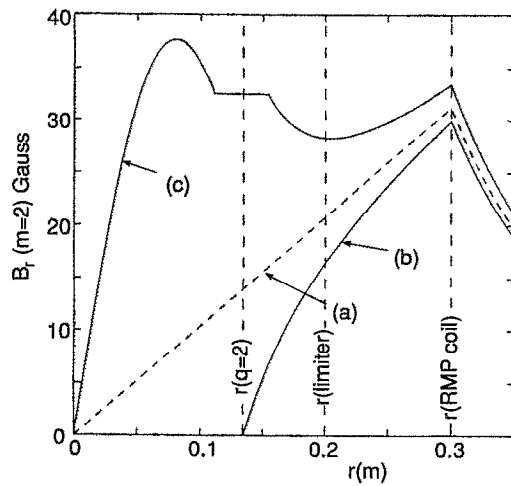


FIG. 2. Solutions of the steady-state tearing-mode equation with helical boundary conditions and no wall. (a): Vacuum field; (b): "untorn"; (c) steady-state torn [$\Delta'(W) = 0$]. Note the difference between the three solutions at the position of a detector outside the plasma. $J_\phi = J_0(-r^2/a^2)^6$, $q(0) = 0.6$ is used: $a\Delta_0(0) = 0.05$ for $m = 2$.

erywhere lower than $b_r^{\text{vac}}(r)$, and this difference may be detected outside the plasma. As the island appears B_r increases. Figure 2 shows the three solutions of the cylindrical low- β tearing mode equation: vacuum, "untorn" (no island), and the appropriate fully reconnected solution after penetration. The final solution satisfies $\Delta'(W) = 0$ where $\Delta'(W) = [\partial \ln(rB_r)/\partial r]_{r_1}^2$. Here B_r matches the helical boundary condition at the RMP coil and the island of width W spans $r_1 < r < r_2$. The equilibrium chosen for Fig. 2 in fact approximately reproduces the magnitude of the reduction and amplification (factor $\sim 2-4$) observed in the experiment before and after penetration [Fig. 1(b)] [no special significance should be attached to the value of $q(0)$ in the model since it is a consequence of the class of profiles chosen—the amplification is controlled mainly by the shape of $J(r)$ in the environs of the magnetic island]. There will be modest corrections (reductions) to the $m = 2, n = 1$ island width due to plasma drag on the locked island¹⁰ and some changes due to toroidicity.¹⁴ The presence in the experiment of only a small island ($W/a \lesssim 3\%$) before application of the RMP is consistent with the profile being near marginal stability. Theoretically the amplification is a function of the stability of the initial equilibrium, and larger for smaller $|\Delta_0(0)|$, but the predicted⁹ singularity in the amplification at $\Delta_0(0) = 0$ does not occur in a nonlinear calculation¹⁴ [$\Delta_0'(W)$ is defined in the same way as $\Delta'(W)$, but for no RMP]. For large induced islands the final island width is not directly related to $\Delta_0(0)$ but is controlled by somewhat larger scale features of the current profile. Experimentally, changes in the amplification are observed for different conditions but these are rather weak, as expected for the large islands induced on COMPASS-C. Another check on $\Delta_0(W)$ is available from the decay rate of the rotating island after the RMP is removed. If this decay is fitted to a nonlinear island evolution model¹⁵

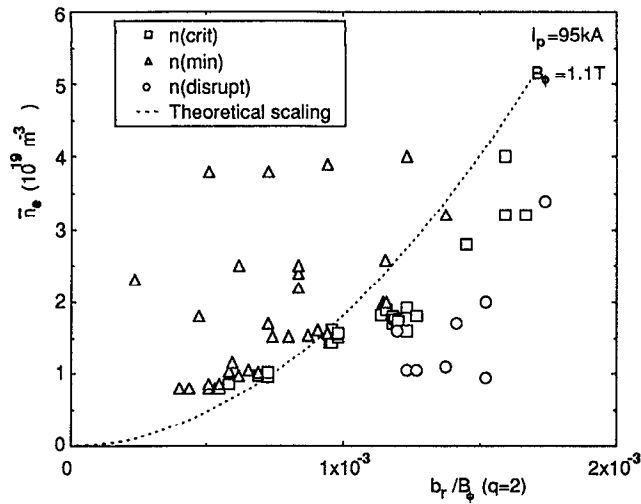


FIG. 3. The penetration threshold as a function of density for $I_p = 95$ kA, $B_\phi = 1.1$ T [$q(a) \approx 4.3$]. Δ : No penetration and the minimum value of \bar{n}_e for constant B_r/B_ϕ ; \square : threshold. A theoretical scaling is also shown (broken line), as are stimulated disruptions (\circ).

$\tau_R d(W/a)/dt \sim a\Delta'_0(W)$ with the resistive time scale τ_R defined as $\mu_0 a^2/\eta_{\parallel}(r_s)$, then $\Delta'_0(W)$ can be deduced, and for a reasonable value of τ_R (~ 50 msec), $\Delta'_0(W)$ fits the values deduced for the natural $\sim 3\%$ island and the initial fully penetrated island.¹⁶

A simplified explanation of the origin of the penetration threshold is as follows. Tearing modes in a normal Ohmic discharge are observed to rotate with a frequency $f_s \approx 14$ kHz, faster than the impurity rotation frequency and on the order of the sum of the electron diamagnetic ($\omega_{*,e}$) and $\mathbf{E} \wedge \mathbf{B}$ frequencies at r_s .¹⁷ A perturbation at frequency f_{RMP} where $|f_{\text{RMP}} - f_s| \gg \gamma$ (the mode growth/damping rate) leads to only a very small island since the mode is being driven off resonance. There is, however, a torque between this small island and the applied field tending to drag f_s to f_{RMP} (which is zero for static RMP's). Above some critical RMP level, this drag leads nonlinearly to complete arrest of the island, and full penetration of the applied perturbation. The threshold is found to be dictated by the plasma inertia and viscosity (including poloidal flow damping) as well as f_s and geometric factors.^{10,16} For typical COMPASS-C parameters, the dominant dependences are given by $B_r^{\text{thresh}}(2,1)/B_\phi = C f_0^{0.7} \rho^{0.5} \tau_\phi^{-0.3} (-r_s \Delta'_0)^{0.5}$, where B_r^{thresh} is the threshold value of $B_r^{\text{vac}}(r_s)$, ρ is the mass density, and τ_ϕ is a global momentum confinement time. While the theory applies to machines of any size, this particular power-law approximation is only valid for a modest range of parameters: the exponents are changed slightly for ITER, for example. The change in fluid velocity at penetration, f_0 , is taken to scale linearly with f_s , with some experimental support. The coefficient C is a predicted geometric factor which is here adjusted to fit the data (to include profile effects for example) and $-r_s \Delta'_0$ is evaluated at the steady-state penetrated island width (it is the solution of a nonlinear equation, with a single well-behaved

positive real root for monotonic Δ_0). In Fig. 3 the experimental threshold is seen to agree well with the predicted \bar{n}_e dependence (minor discrepancies can arise through indirect n_e dependences). The theoretical curve is evaluated with τ_ϕ, Δ'_0 constant: the amplification of the applied RMP by the plasma is not observed to change significantly with \bar{n}_e , so $\Delta'_0 = \text{const}$ is a reasonable approximation. Also shown in this figure are points corresponding to stimulated disruptions; they occur close to the penetration points because of the relatively high value of $B_r^{\text{thresh}}(2,1)/B_\phi$ on COMPASS-C. It is also found that penetration and stimulated disruptions occur at lower RMP levels for lower $q(a)$, an effect that is mainly due to the r^{n-1} variation of the applied field. In addition, applying an RMP at the start of the discharge did not lead to a sustained stationary island in the current rise—this is understood if the $q = 2$ surface first appears at the magnetic axis, when scenarios can be constructed with $B_r^{2,1}(q = 2)$ remaining below the threshold as the discharge grows.

Since arrest of the $m = 2$ island during the penetrated phase is predicted, measurements of the fluid rotation are of interest. Experimentally, the change in v_ϕ^{imp} coincides with the penetration; also the recovery of the mode and impurity velocities to their unperturbed values after removal of the RMP have identical time dependence, thus providing compelling support for the model. The magnitude of the change in v_ϕ^{imp} is in fact only about half of the initial value of $2\pi R f_s$; this may be due to a reduction in $\omega_{*,e}$ as the profiles are modified by the induced island, or else shear in $v_\phi^{\text{imp}}(r)$. The reversal in v_ϕ^{imp} is expected; a relative velocity between the island and fluid frames will remain when the island is locked to the RMP frame.

Figure 1(b) shows one more important effect: there is “hysteresis” in the mechanism. The RMP level at unlocking is less (by a factor ~ 2 when I_{RMP} is reduced slowly) than that at penetration. One explanation is that at penetration only a region of fluid close to the $q = 2$ surface is slowed, with correspondingly large viscous forces opposing the local change in velocity, whereas at unlocking the velocity perturbation has diffused, so the viscous force opposing the mode-lock force is reduced and can be balanced by a smaller RMP. Since the density appears in the expression for the penetration point, a density threshold for constant RMP level is predicted and observed: reducing \bar{n}_e results in penetration (on DIII-D¹ as well as COMPASS-C). It is found that hysteresis also applies to the density threshold: increasing \bar{n}_e by up to a factor 2 during the locked period does not lead to unlocking—in fact unlocking by this method has not been observed on COMPASS-C. For unlocking to occur with increasing \bar{n}_e , the viscous drag between the fluid frame and the locked mode frame must increase with density to overcome the mode-locking force, or else the mode-locking force must decrease due to a reduction in W , either through inertial stabilization¹⁰ or due to a change in Δ'_0 , and so this hysteresis is not unexpected.

C. RMP's with other helicities

The same basic phenomena are observed when 3,2 and 4,2 RMPs are applied to similar discharges. Again the impurity rotation is changed, by a similar amount, although for the 3,2 RMP, the BIV emission originates ~ 5 cm from the primary resonant surface. Together with the observation of very slow (~ 1 kHz) $m = 2, n = 1$ oscillations this suggests that a large fraction of the plasma is indeed slowed as indicated by the hysteresis effect described above. The 2,1 RMP's lead to removal of the sawtooth at the time of penetration (Fig. 1), but the 3,2 and 4,2 perturbations do not. A 1,1 perturbation, on the other hand, has very little effect even for B_r^{vac} ($m = 1, n = 1$) as high as 30 G. As $I_{\text{RMP}}^{m=1, n=1}$ is raised, penetration and disruptions are eventually observed, but this is believed to be due to penetration of the 2,1 sideband (produced by toroidal effects).

III. CONCLUSIONS

In summary, Ohmic discharges in COMPASS-C have been used to verify a model for the penetration of error fields into tokamaks, where full penetration does not occur if the frame of the tearing mode rotates with respect to the error field. It is found that there is a sharp threshold in the error field level, B_r^{thresh} (applied, $q = 2$)/ B_ϕ , and the threshold increases with density in accordance with the model. Rotation measurements with submillisecond time resolution confirm that the plasma rotation changes as the island is formed. The model explains why small tokamaks which rotate fast are apparently insensitive to coil misalignments: B_r^{thresh} (applied)/ $B_\phi \sim 2 \times 10^{-3}$ for COMPASS-C, while a level of $\sim 10^{-5}$ is predicted for OH discharges in the larger ITER device ($R = 6$ m), using $f_0 = 170$ Hz, $n = 3 \times 10^{19} \text{ m}^{-3}$, $\tau_\phi = 3.8$ sec. The theoretical model suggests that the error field level that leads to magnetic islands can be raised by injection of momentum.

ACKNOWLEDGMENTS

The authors would like to acknowledge contributions from D. C. Robinson, J. Hugill, and R. J. La Haye. They are also grateful for the assistance of the whole COMPASS-C team.

- ¹J. T. Scoville, R. J. La Haye, A. G. Kellman, T. H. Osborne, R. D. Stambaugh, E. J. Strait, and T. S. Taylor, Nucl. Fusion **31**, 875 (1991).
- ²F. Karger, H. Wobig, S. Corti, J. Gernhardt, O. Klüber, G. Lisitano, K. McCormick, D. Meisel, and S. Sesnic, in *Proceedings of the Fifth International Conference on Plasma Physics and Controlled Nuclear Fusion Research*, Tokyo (IAEA, Vienna, 1975), Vol. 1, p. 207.
- ³K. Bol, J. L. Cecchi, C. C. Daughney, F. DeMarco, R. A. Ellis, Jr., H. P. Eubank, H. P. Furth, H. Hsuan, E. Mazzucato, and R. R. Smith, in Ref. 2, p. 83.
- ⁴J. J. Ellis, A. A. Howling, A. W. Morris, and D. C. Robinson, in *Proceedings of the Tenth International Conference on Plasma Physics and Controlled Nuclear Fusion Research*, London (IAEA, Vienna, 1985), Vol. 1, p. 363.
- ⁵A. W. Morris, R. Fitzpatrick, P. S. Haynes, T. C. Hender, J. Hugill, C. Silvester, and T. N. Todd, in *Proceedings of the 17th European Conference on Controlled Fusion and Plasma Heating*, Amsterdam (EPS, Petit-Lancy, Switzerland, 1990), Vol. 14B, Part II, p. 379.
- ⁶A. W. Morris, S. A. Arshad, T. Edlington, S. J. Fielding, G. M. Fishpool, P. S. Haynes, T. C. Hender, J. Hugill, I. Jenkins, P. C. Johnson, B. Lloyd, M. O'Brien, A. C. Riviere, D. C. Robinson, C. Silvester, E. J. Strait, T. N. Todd, and C. D. Warrick, in *Proceedings of the Thirteenth International Conference on Plasma Physics and Controlled Nuclear Fusion Research*, Washington, DC (IAEA, Vienna, 1991), Vol. 1, p. 797.
- ⁷D. E. Roberts, D. Sherwell, J. D. Fletcher, G. Nothnagel, and J. A. M. de Villiers, Nucl. Fusion **31**, 319 (1991).
- ⁸J. Chen, J. Xie, Y. Huo, L. Li, Q. Zhao, G. Zhang, M. Wang, D. Guo, Q. Guo, P. Qin, G. Li, H. Fan, C. Deng, X. Tong, and R. Huang, Nucl. Fusion **30**, 2271 (1990).
- ⁹J. K. Lee, H. Ikezi, F. W. McClain, and N. Ohyabu, Nucl. Fusion **23**, 63 (1983).
- ¹⁰R. Fitzpatrick and T. C. Hender, Phys. Fluids B **3**, 644 (1991).
- ¹¹R. J. Hayward, P. J. Crawley, R. T. Crossland, B. S. Ingram, A. P. Pratt, and R. T. C. Smith, in *Proceedings of the 15th Symposium on Fusion Technology*, Utrecht, 1988 (North-Holland, Amsterdam, 1989), Vol. 1, p. 361.
- ¹²K. Tomabechi and the ITER team, in Ref. 6.
- ¹³R. T. Crossland, R. J. Hayward, T. N. Todd, P. S. Haynes, J. W. Hill, A. W. Morris, P. Nicholson, and R. A. Crook, in *Proceedings of the 16th Symposium on Fusion Technology*, London, 1990 (Pergamon, New York, 1991), Vol. 1, p. 632.
- ¹⁴A. Reiman and D. Monticello, Phys. Fluids B **3**, 2230 (1991).
- ¹⁵P. H. Rutherford, Phys. Fluids **16**, 1903 (1973).
- ¹⁶T. C. Hender, R. Fitzpatrick, A. W. Morris, P. S. Haynes, I. Jenkins, D. C. Robinson, and T. N. Todd, in *Proceedings of the 18th European Conference on Controlled Fusion and Plasma Physics*, Berlin (EPS, Petit-Lancy, Switzerland, 1991), Vol. 4, p. 77.
- ¹⁷O. Klüber, H. Zohm, H. Bruhns, J. Gernhardt, A. Kallenbach, and H. P. Zehrfeld, Nucl. Fusion **31**, 907 (1991).